Chemistry Europe
European Chemical Societies Publishing

WILEY VCH

Excellence in Chemistry Research

Announcing our new flagship journal

- Gold Open Access
- Publishing charges waived
- Preprints welcome
- Edited by active scientists

Meet the Editors of *ChemistryEurope*

Luisa De Cola
Università degli Studi di Milano Statale, Italy

Ive Hermans
University of Wisconsin-Madison, USA

Ken Tanaka
Tokyo Institute of Technology, Japan

Check for updates

EurJIC
European Journal of Inorganic Chemistry

Research Article
doi.org/10.1002/ejic.202300375

Chemistry Europe
European Chemical Societies Publishing

www.eurjic.org

Cerium(IV) Nitrate Complexes With Bidentate Phosphine Oxides

Simon J. Coles,[a] Simon Cooper,[b] Wim T. Klooster,[a] Laura J McCormick Mc Pherson,[a] and Andrew W. G. Platt*[b]

The reactions between ceric ammonium nitrate, $(NH_4)_2Ce(NO_3)_6$, (CAN) and the bidentate phosphine oxides, 4,5-bis(diphenylphosphine oxide)-9,9-dimethylxanthene (L^1), oxydi-2,1-phenylene bis(diphenylphosphine dioxide) (L^2), 1,2-bis(diphenylphosphino)ethane dioxide (L^3) and 1,4-bis(diphenylphosphino)butane dioxide, L^4 have been investigated. The crystal structures of the molecular $Ce(NO_3)_4L^1$ (**1**), and ionic $[Ce(NO_3)_3L^3{}_2][NO_3]\cdot CHCl_3$ (**3**), $[Ce(NO_3)_3L^3{}_2][NO_3]$ (**4**) and the polymeric $[Ce(NO_3)_3L^4{}_{1.5}]$ $[NO_3]$ (**5**) and the cerium(III) complex $[Ce(NO_3)_2L^1{}_2][NO_3]$ (**2**) are reported. The thermal stability of the complexes has been examined by thermogravimetry with the gaseous decomposition products analysed by infrared spectroscopy. Evolution of CO_2 is found for both Ce(III) and Ce(IV) complexes with the later also forming NO_2. The formation of the complexes in solution has been studied by ^{31}P NMR spectroscopy and further complexes $[Ce(NO_3)_3L^1{}_2]^+$ $[NO_3]^-$ and $[Ce(NO_3)_2L^1{}_3]^{2+}2[NO_3]^-$ identified in CD_3CN solution. The complex (**1**) exists as a single molecular species in solution and is stable in dichloromethane whilst (**3**) decomposes on standing in both CD_2Cl_2 and CD_3CN to Ce(III) containing species. Complexes of L^2 have been identified by solution ^{31}P NMR spectroscopy and these decompose in solution to give $Ce(NO_3)_3L^2{}_2$. This study represents the first structural characterisations of Ce(IV) complexes with bidentate phosphine oxides.

Introduction

The coordination chemistry of cerium(IV) has been studied in detail as it serves as a mimic for plutonium(IV) systems,[1,2] because of the catalytic properties of its complexes, [3,4] their use as photocatalysts,[5,6] one electron oxidants[7,8, 9] and in the extraction of Ce(IV) from aqueous media.[10] Its coordination chemistry with phosphine oxides, however, is relatively unexplored.[11,12] Since the initial and subsequent reports of $Ce(NO_3)_4(Ph_3PO)_2$[13,14] there have been few reports of phosphine oxide complexes. A thermally unstable complex with $Ph_2P(O)CH_2C(O)Ph$ was isolated and characterised as $Ce(NO_3)_3(Ph_2P(O)CHC(O)Ph)(Ph_2P(O)CH_2C(O)Ph)_2$ on the basis of elemental analysis and infrared spectroscopy.[15] The cerium(IV) complex, $Ce(NO_3)_4(^tBuPhPOC_2H_4POPh^tBu)$ was prepared from ceric ammonium nitrate, $(NH_4)_2Ce(NO_3)_4$ (CAN), and the ligand in acetone and characterised by spectroscopy and elemental analysis but the structure was not reported.[16] The Ce(III) complex $Ce(NO_3)_3((n\text{-}C_8H_{17})PhP(O)CH_2N^iBu_2)_3$ undergoes reversible one electron oxidation in acetonitrile solution but the Ce(IV) complex formed was not further characterised.[17] Cerium(IV) nitrate complexes with trialkylphosphine oxides have been reported more recently with $Ce(NO_3)_4(Cy_3PO)_2$ having a similar structure to the Ph_3PO analogue, whilst with Et_3PO a cationic complex, $[Ce(NO_3)_3(Et_3PO)_3]^+$, was structurally characterised.[18] Complexes with bidentate ligands have not been reported and we report here our investigations into the reactions of CAN with various bidentate phosphine oxide ligands and the structures of complexes of cerium(IV) nitrate with 4,5-bis(diphenylphosphine oxide)-9,9-dimethylxanthene (L^1), oxydi-2,1-phenylene bis(diphenylphosphine dioxide) (L^2), 1,2-bis(diphenylphosphino)ethane (L^3) and cerium(III) complexes with L^1 and 1,4-bis(diphenylphosphino)butane, (L^4). The ligand structures are shown in Figure 1

The choice of ligands was made on the basis of the differing flexibilities of the linker architecture between the two phosphine oxide groups, with L^1 having limited flexibility whilst L^2, L^3 and L^4 have more scope to accommodate different geometries on coordination to the metal. This study aims to examine effect of this on the formation and stability of the Ce(IV) complexes.

Results and Discussion

The complexes $Ce(NO_3)_4L^1$ (**1**) and $[Ce(NO_3)_3L^4{}_{1.5}]$ (**5**) were obtained from the reaction of chlorocarbon solutions of the ligand with solid CAN. Complexes $[Ce(NO_3)_3L^3{}_2]NO_3\cdot CHCl_3$ (**3**),

[a] Prof. S. J. Coles, Dr. W. T. Klooster, Dr. L. J McCormick Mc Pherson
UK National Crystallography Service
Department of Chemistry, University of Southampton
Highfield Campus
Southampton, SO17 1BJ (UK)

[b] S. Cooper, Dr. A. W. G. Platt
School of Justice
Security and Sustainability,Staffordshire University
Science Centre, Leek Road
Stoke on Trent, ST4 2DF (UK)
E-mail: a.platt@staffs.ac.uk

Supporting information for this article is available on the WWW under https://doi.org/10.1002/ejic.202300375

© 2023 The Authors. European Journal of Inorganic Chemistry published by Wiley-VCH GmbH. This is an open access article under the terms of the Creative Commons Attribution Non-Commercial NoDerivs License, which permits use and distribution in any medium, provided the original work is properly cited, the use is non-commercial and no modifications or adaptations are made.

© 2023 The Authors. European Journal of Inorganic Chemistry published by Wiley-VCH GmbH

Research Article
doi.org/10.1002/ejic.202300375

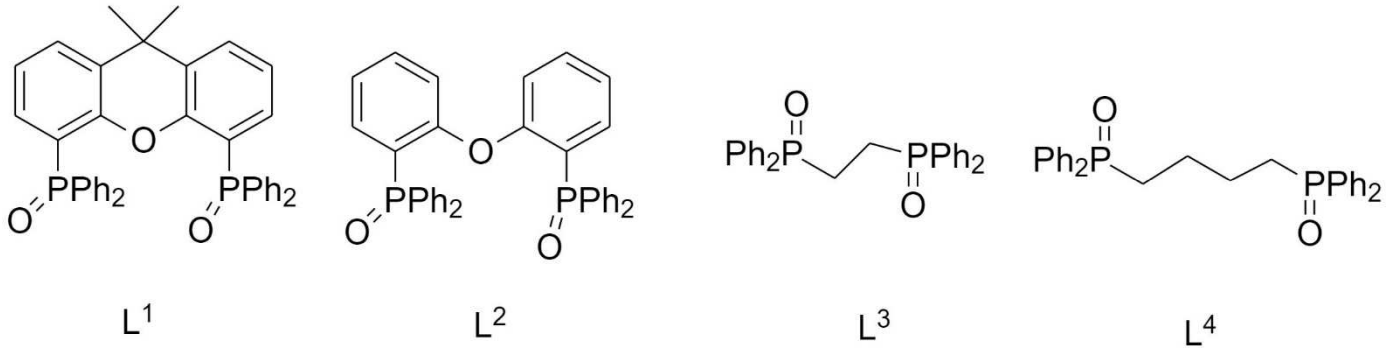

Figure 1. The structures of the ligands.

$[Ce(NO_3)_3L^3{}_2]NO_3$ (**4**), and an impure Ce(IV) complex with L^2, were prepared by the biphasic reaction of aqueous CAN with chlorocarbon solutions of L^2 and L^3. The Ce(III) complex $[Ce(NO_3)_2L^1{}_2]^+[NO_3]^-$, (**2**) was prepared by the reaction of $Ce(NO_3)_3{\cdot}6H_2O$ with L^1 in hot ethanol. All of the isolated solids are stable to air and moisture at ambient temperature as evidenced by their infrared and NMR spectra remaining unchanged on prolonged exposure to normal laboratory conditions. Similarly no special measures were to taken to exclude air and moisture from samples submitted for elemental analysis. The reaction of CAN with 2 equivalents of L^1 led to the isolation of a solid which contained predominantly $Ce(NO_3)_4L^1{}_2$ in addition to a small amount of (**1**), unreacted L^1 and (**2**) (NMR evidence), but attempts to obtain crystals suitable for structural work were not successful.

Attempts to obtain crystals of complexes of L^2 were similarly not successful due to the low solubility of the Ce(III) and Ce(IV) complexes in all common organic solvents. The Ce(IV) complex of L^2 is slightly soluble in CD_2Cl_2 and CD_3CN. Slow evaporation of CH_2Cl_2 solutions led to the formation of $Ce(NO_3)_3L_2{}^2$ which had identical infrared and ^{31}P NMR spectra to a sample prepared from $Ce(NO_3)_36H_2O$ and L^2 from ethanol.

The infrared spectra of all complexes are typical of phosphine oxide - lanthanide nitrate complexes.[19] The bands due to coordinated nitrate are generally easily identified with the exception of complexes of L^1 for which the ν_4 and ν_5 absorptions are obscured by ligand peaks. The assignments of the main bands are given in Table S1. The presence of ionic nitrate was not apparent in the spectra of (**2**), (**3**) or (**4**). In the case of (**2**) this is clearly due to a lowering of the local symmetry on hydrogen bonding to ethanol. In (**3**) and (**4**) the ionic nitrate is present in the lattice with reduced local symmetry.

Thermal Stability

The thermal stability of L^1, (**1**), (**2**) and (**3**) was examined by thermogravimetric analysis under a nitrogen atmosphere from 30–1000 °C with the infrared spectra of the volatile

decomposition products monitored at each mass loss. The results are summarised in Table 1 and illustrated for (**1**) in Figure 2. The TGA results for all the complexes studied are given in Figure S1. The cerium(IV) complexes (**1**) and (**3**) decompose at lower temperatures leading to the evolution of NO_2 and CO_2 (and the lattice $CHCl_3$ in the case of (**3**)) with no NO_2 detected during the decomposition of (**2**). Potassium cerium(IV) nitrate can act as a source of the highly oxidising nitrate radical under photolysis in CH_3CN[20] but there are no reports of this being generated under thermal conditions. A Ce(III) complex is formed as an intermediate during the thermal decomposition of $K_2Ce(NO_3)_6$ and $Rb_2Ce(NO_3)_6$ with the formation of nitric oxide, nitrogen dioxide and oxygen where the oxidation of a nitrate oxygen by Ce^{4+} is thought to occur,[21,22] A similar process may be occurring here leading to the simulta-

Table 1. Thermogravimetric analysis of L^1, (**1**), (**2**), and (**3**).

$L^1.H_2O$		$Ce(NO_3)_4L^1$ (**1**)		$Ce(NO_3)_3L^1{}_2$ (**2**)		$[Ce(NO_3)_3L^2{}_2][NO_3]CHCl_3$ (**3**)	
Temperature/ °C (mass loss %)	Gaseous decomposition products[a,b]	Temperature/ °C (mass loss %)	Gaseous decomposition products	Temperature/ °C (mass loss %)	Gaseous decomposition products	Temperature/ °C (mass loss %)	Gaseous decomposition products
						121 (9)	$CHCl_3$,CO_2, NO_2, H_2O
		241 (11)	CO_2, NO_2, H_2O				
		358 (15)	CO_2 H_2O	371 (22)	CO_2, H_2O, $L^{[1a]}$	343 (34)	CO_2, N_2O H_2O
425 (100)	L,[1a] H_2O[a]	405 (16)	CO_2, H_2O	424 (47)	$L^{[1]}$		
		618 (12)	$L^{[1]}$	624 (8)	$L^{[1]}$	582 (27)	

[a] Identified by infrared spectrum.

© 2023 The Authors. European Journal of Inorganic Chemistry published by Wiley-VCH GmbH

10990682c, 0 Downloaded from https://chemistry-europe.onlinelibrary.wiley.com/doi/10.1002/ejic.202300375 by University Of Southampton, Wiley Online Library on [03/11/2023]. See the Terms and Conditions (https://onlinelibrary.wiley.com/terms-and-conditions) on Wiley Online Library for rules of use; OA articles are governed by the applicable Creative Commons License

Research Article
doi.org/10.1002/ejic.202300375

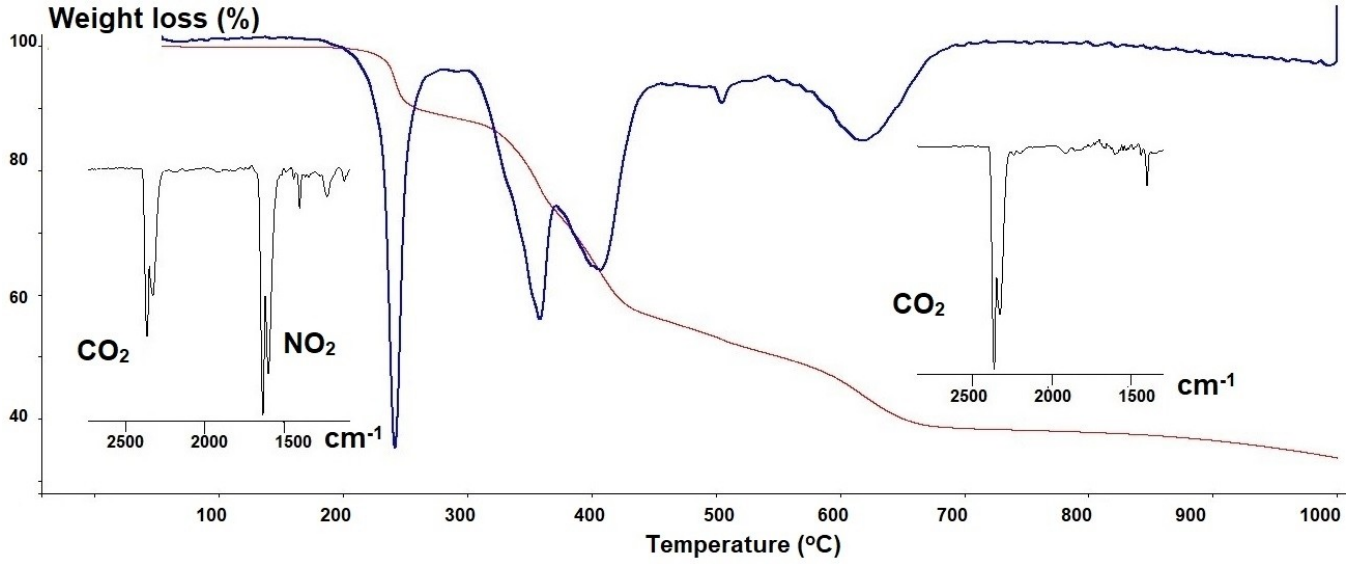

Figure 2. The TGA curve (red) and the derivative (blue) for (**1**). The insets show the infrared spectra of gaseous products formed at 250 °C and 350 °C respectively.

neous reduction to Ce^{3+} and oxidation of the hydrocarbon periphery of the ligand to generate the observed CO_2, NO_2 and H_2O. The behaviour at higher temperatures is very similar with both Ce(IV) and Ce(III) species further decomposing to give CO_2, presumably by nitrate oxidation followed by liberation of L^1 at around 620 °C (compared with 425 °C for L^1 itself) in the case of (**1**) and (**2**). Previous stidies on the thermogravimetric analysis of several metal nitrates, including cerium and gadolinium, found that NO_2 and O_2 were evolved in air, whilst in a reducing H_2 atmosphere the gaseous products were N_2 and H_2O.[23] For the Ce complexes here, the presence of the hydrocarbon moieties in the ligand would provide a reducing environment for the thermal decomposition of the remaining nitrate ions and hence the formation of CO_2, water and presumably N_2 as the nitrogen containing product of nitrate reduction.

$L^1.H_2O$ itself shows a single 100% mass loss at 425 °C presumably due to boiling.

In all cases the solid residue from the decomposition of the complexes was a black intractable material whose infrared spectrum showed a strong, broad absorption with peak maxima at 1084, 990, 951 and 907 cm^{-1} which are consistent with the spectra of coordinated phosphate ion.[23,24]

Crystal Structures

General points

Some general aspects are discussed followed by comments specific to the individual structures. The crystal structures of five complexes were determined by single crystal x-ray diffraction and details of the data collection and refinement are given in the supplementary information. The full listing of bond distances and angles are given in Tables S2 and S3 respectively in the supplementary information. Apart from (**5**) which is polymeric, the compounds crystallise with discreate molecules or ions in the lattice. There are no significat Ce….Ce interactions with the distance between adjacent metals in the lattice being over 10 Å in all cases. There are weak intermolecular interactions between adjacent moleclues in all of the structures. These take the form of weak hydrogen between coordinated nitrate oxygen atoms and the hydrogens of the aromatic rings of neighbouring molecules or ions C–H….O generally in the region of 2.36 to 2.55 Å. The ionic nitrate ions in (**2**), (**3**) and (**4**) also weakly interact with the aromatic C–H groups. The geometries around the cerium ions were determined by continuous shape measures[25,26] which gives the sum of squares (S) of deviations of the coordinated atoms from their positions in idealised polyhedra. Values of S between 0.1 and 3 represent small distortions from the optimum geometry with higher values being indicative of more significant deviations. The S values are also included in Table S2 and are generally in the acceptable range for the assigned geometry.

The average Ce–O bond distances are given in Table 2 together with the calculated oxidation states for the complexes. Assignment of oxidation states to cerium complexes is often not straightforward.[28] The use of bond valence sums in this regard can prove useful and we have previously used this to show that $[Ce(NO_3)_3(Et_3PO)_3]^+$ is indeed a cerium(IV) complex.[18]

Table 2. Average Ce–O bond distances (Å) and calculated oxidation states for complexes (**1**) to (**5**).

Complex	(**1**)	(**2**)	(**3**)	(**4**)	(**5**)
Ce–O	2.43(11)	2.48(11)	2.43(11)	2.43(10)	2.47(10)
Ce–O(N)	2.48(5)	2.58(2)	2.51(4)	2.51(3)	2.541(6)
Ce–O(P)	2.244(8)	2.39(1)	2.31(2)	2.31(2)	2.336(1)
OS(+3)[a]	4.49	3.09	4.43	4.49	3.58
OS(+4)[a]	3.95	2.72	3.89	3.95	3.14

© 2023 The Authors. European Journal of Inorganic Chemistry published by Wiley-VCH GmbH

10990682c, 0 Downloaded from https://chemistry-europe.onlinelibrary.wiley.com/doi/10.1002/ejic.202300375 by University Of Southampton, Wiley Online Library on [03/11/2023]. See the Terms and Conditions (https://onlinelibrary.wiley.com/terms-and-conditions) on Wiley Online Library for rules of use; OA articles are governed by the applicable Creative Commons License

Research Article
doi.org/10.1002/ejic.202300375

The results in Table 2, with the exceptions of (**2**), which was synthesised from Ce(III) starting materials, and (**5**) (discussed below) are in good agreement with the assignments of the oxidation states as Ce(IV). The average Ce–O bond distances are also in accord with these conclusions with complexes (**1**), (**3**) and (**4**) having average values of 2.43 (10) Å compared with the literature value of 2.44(3) Å for 10 coordinate Ce(IV).[29] The cerium(III) complex (**2**) has an average Ce–O distance of 2.48(10) Å which is smaller than the literature average of 2.60(10) Å for 10-coordinate complexes. However the average lies well within the rather large range for Ce(III) (2.343 – 2.929 Å.

$$\text{From ref 28 } OS(+3) = \sum_i e^{\frac{2.118-ri}{0.37}}\ OS(+4) = \sum_i e^{(2.07-ri)/0.37} \quad (1)$$

Structures of $Ce(NO_3)_4L^1$ (1) and $[Ce(NO_3)_2L^1{}_2][NO_3]$ (2)

A 1:1 complex of composition $Ce(NO_3)_4L^1$ (**1**) forms on reaction with an excess of solid $(NH_4)_2Ce(NO_3)_6$ with a solution of L^1 in CH_2Cl_2. The complex crystallised in the *P*-1 space group and the molecular structure is shown in Figure 3a. The coordination geometry around the cerium ion is a sphenocorona with a 2, 4, 2, 2 distribution of oxygen atoms around the cerium ion with the phosphine oxide oxygens O13 and O14 forming one of the "2" groups and the nitrate oxygens the remainder as illustrated in Figure 3b.

$$\text{From ref 28 } OS(+3) = \sum_i e^{\frac{2.118-ri}{0.37}} \quad (2)$$

$$OS(+4) = \sum_i e^{(2.07-ri)/0.37} \quad (3)$$

The P=O distances in (**1**) at 1.498 Å are larger than those found in $L^1{\cdot}H_2O$ (1.478(4) Å,[30] as expected, but similar to those in complexes with trivalent lanthanides; in halo complexes of lanthanum (1.485 Å)[31] and complexes with substituted pentane-2,4-dionates of samarium and europium (1.496 Å)[32,33] and do not seem to be lengthened significantly on coordination to the more highly charged ion. The bite angle (O–Ce-O) is 77.4(3)° which is larger than those for L^1 in complexes with trivalent ions where the bite angles range between 70.8–74.7° with an average of 73.1°.

For comparison with the structure of (**1**) $Ce(NO_3)_3L^1{}_2$ (**2**) was prepared. It crystalises in the $P2_1/n$ space group and has an 8-coordinate ionic structure $[Ce(NO_3)_2L^1{}_2]^+[NO_3]^-$ which is shown in Figure 4.

The geometry around the Ce ion is a distorted dodecahedron (S = 3.17). The ionic nitrate is hydrogen bonded to a lattice ethanol molecule (O….O 2.84 Å). The P=O and N–O(Ce) bond distances in (**2**) are shorter than for (**1**) as expected on coordination to a Ce^{3+} compared to Ce^{4+} ion. The intra-ligand O….O distance of 3.040 Å is considerably longer than that found in (**1**) (2.085 Å) and the (P)O–Ce–O(P) bite angle is wider (79.35° in (**2**) compared with 77.35° in (**1**)) reflecting the stronger bonding to the Ce(IV) centre.

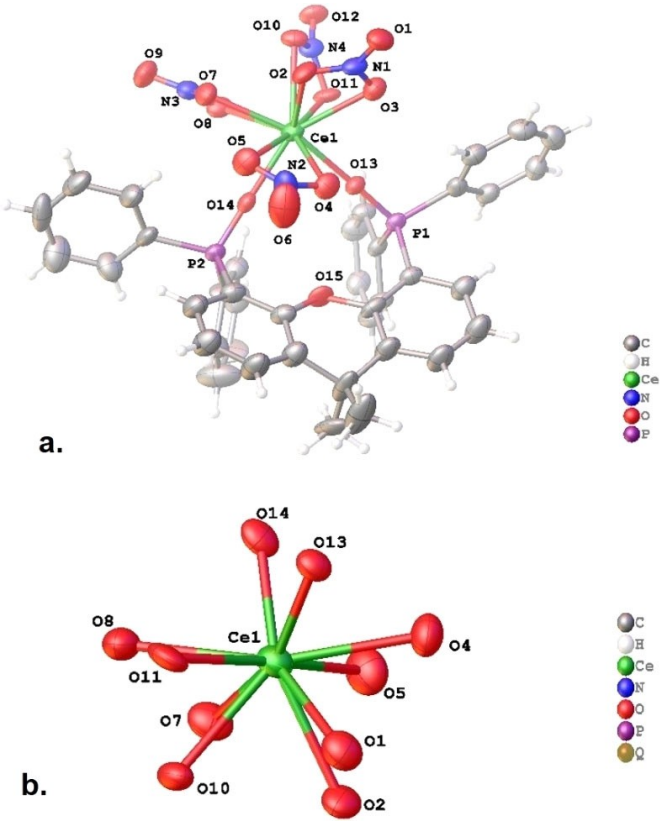

Figure 3. (a) The molecular structure of Ce $(NO_3)_4$ L^1 (**1**). Thermal ellipsoids drawn at 50% (b) the primary coordination sphere illustrating the 2,4,2,2 sphenocorona geometry around the cerium ion.

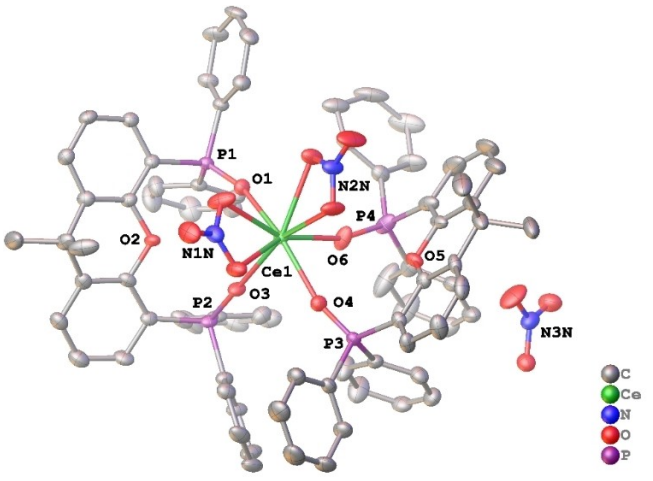

Figure 4. The structure of $[Ce(NO_3)_2L^1{}_2]^+[NO_3]^-$ (**2**). Hydrogen atoms omitted for clarity. Thermal ellipsoids drawn at 50%.

© 2023 The Authors. European Journal of Inorganic Chemistry published by Wiley-VCH GmbH

10990682c, 0 Downloaded from https://chemistry-europe.onlinelibrary.wiley.com/doi/10.1002/ejic.202300375 by University Of Southampton, Wiley Online Library on [03/11/2023]. See the Terms and Conditions (https://onlinelibrary.wiley.com/terms-and-conditions) on Wiley Online Library for rules of use; OA articles are governed by the applicable Creative Commons License

Research Article
doi.org/10.1002/ejic.202300375

10990682c, 0 Downloaded from https://chemistry-europe.onlinelibrary.wiley.com/doi/10.1002/ejic.202300375 by University Of Southampton, Wiley Online Library on [03/11/2023]. See the Terms and Conditions (https://onlinelibrary.wiley.com/terms-and-conditions) on Wiley Online Library for rules of use; OA articles are governed by the applicable Creative Commons License

Structures of $[Ce(NO_3)_3L^3_2][NO_3]$ (3) and (4)

The $[Ce(NO_3)_3L^3_2][NO_3]$ complexes (**3**) and (**4**) crystallise in the $P2_1/c$ space group from either $CHCl_3$ or CD_2Cl_2, with a 10-coordinate Ce ion bound to 2 bidentate phosphine oxides and three nitrate ions with the remaining nitrate not coordinated to the metal. The assignment of the complex as Ce(IV) is further supported by an analysis of the bond distances (see Table 2), and from the fact that the $Pr(NO_3)_3$ complex with L^3 has a polymeric structure[34] rather than the mononuclear structure found here.

The complex crystallised from CD_2Cl_2 has a geometry best described a 2,4,2,2 sphenocorona (S = 2.9) although when crystallised from $CHCl_3$ a bicapped square antiprism is a marginally better description. In both cases the differences in S-values between the sphenocorona and bicapped square antiprism are small and either description appears adequate. The structure of the complex is shown in Figure 5a and the core structure illustrating the bicapped square antiprism in Figure 5b.

The structure is very similar to the analogous thorium(IV) complex, $[Th(NO_3)_3L^3_2]^+[NO_3]^-$[35] which also has a bicapped square antiprismatic coordination geometry. The bond distances and angles are also very similar between the thorium complex and the two cerium(IV) analogues reported here. The bite angles of both nitrate and phosphine oxide ligands are slightly larger for Ce^{4+} possibly due to the difficulty in a small bite angle ligand such as nitrate accommodating the smaller ionic radius. A schematic comparison of the bond distances and angles is given in Figure S2 in the supplementary information.

There is a pseudo meridonal arrangement of nitrate ligands (considering the NO_3^- to be a monodentate ligand bonded via the N-atom) which is also seen in $Ln(NO_3)_3$/phosphine oxide complexes but not in $[Ce(NO_3)_3(Et_3PO)_3]^+$[18] where the nitrates adopt a pseudo *fac*-arrangement. In (**3**) and (**4**) a *fac*-arrangement of nitrates would be less favourable as this would necessitate bringing the two bulky chelating ligands into a pseudo *cis* – geometry and thus into closer proximity increasing unfavourable steric interactions.

Structure of $Ce(NO_3)_3L^4_{1.5}[NO_3]$ (5)

The complex (**5**) formed during the reaction of CAN with L^4 in CD_2Cl_2, crystallises in the *P*-3*c*1 space group with a polymeric network of $Ce(NO_3)_3L^4_{1.5}$ units linked by ligands bridging between two metal centres (rather than chelating) as shown in Figure 6. The geometry around the cerium ions as a tricapped trigonal prism (S = 2.5) and this together with the asymmetric unit for the structure are shown in Figures 7 a and b respectively.

The trigonal planes are parallel and the angles between the square faces (each defined by two O1 and two O4 atoms) at 60.03° are almost identical to the idealised geometry. The solution of the structure gave a residual electron density of 32 electrons, very close to the 31 expected for a nitrate ion. This implies that (**5**) may be a Ce(IV) complex. The average Ce–O length of 2.47(10) Å lies between the 9-coordinate averages of 2.55(10) Å for Ce(III) and 2.34(6) for Ce(IV) and comfortably within the range for either oxidation state.[29] Oxidation state calculations are similarly inconclusive (Table 2), a situation which has previously been taken as an indication of the presence of both Ce(III) and Ce(IV) in the structure,[28] although we find no evidence of inequivalent cerium environments in

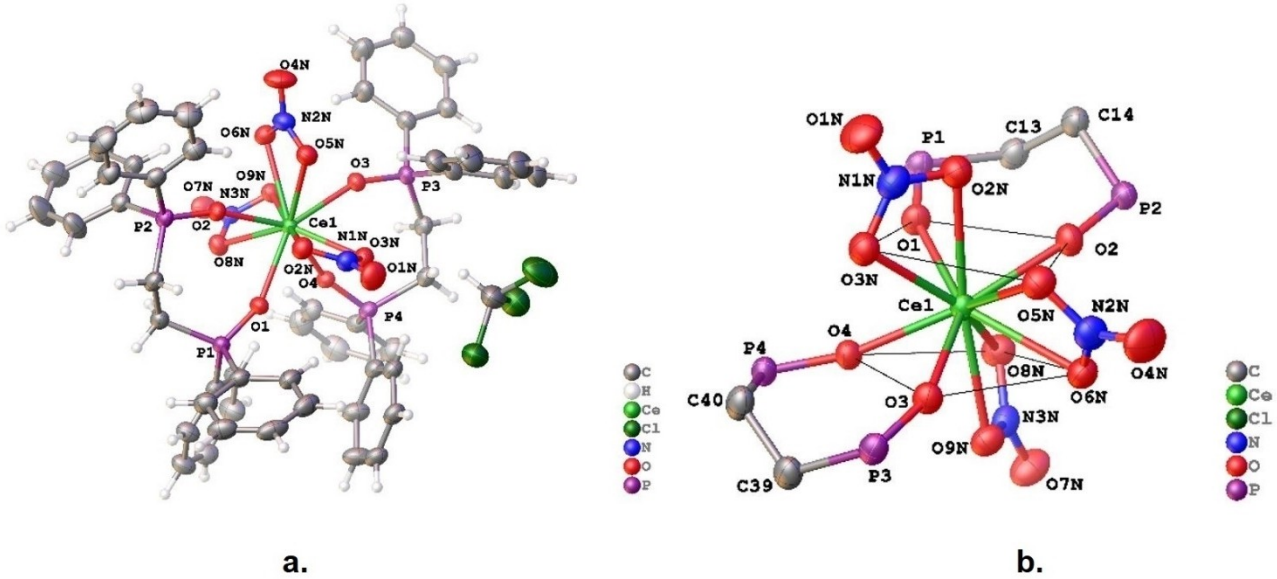

Figure 5. (a) The molecular geometry of the $[Ce(NO_3)_3L^3_2]^+ \cdot CHCl_3$ cation in (**3**). Thermal ellipsoids drawn at 50%. (b) The bicapped square antiprism core geometry (hydrogen atoms and phenyl rings omitted for clarity.

© 2023 The Authors. European Journal of Inorganic Chemistry published by Wiley-VCH GmbH

Research Article
doi.org/10.1002/ejic.202300375

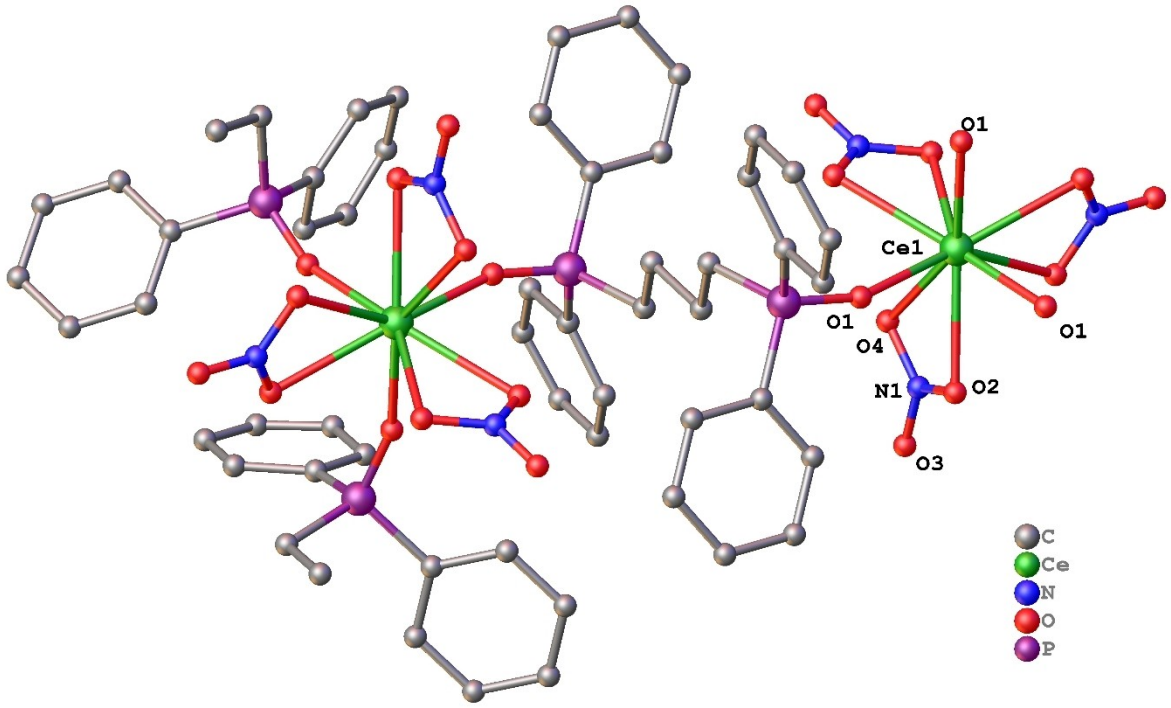

Figure 6. The structure of $Ce(NO_3)_3L^4_{1.5}$ (**5**) showing the atom labelling of the coordination sphere. Hydrogen atoms omitted for clarity.

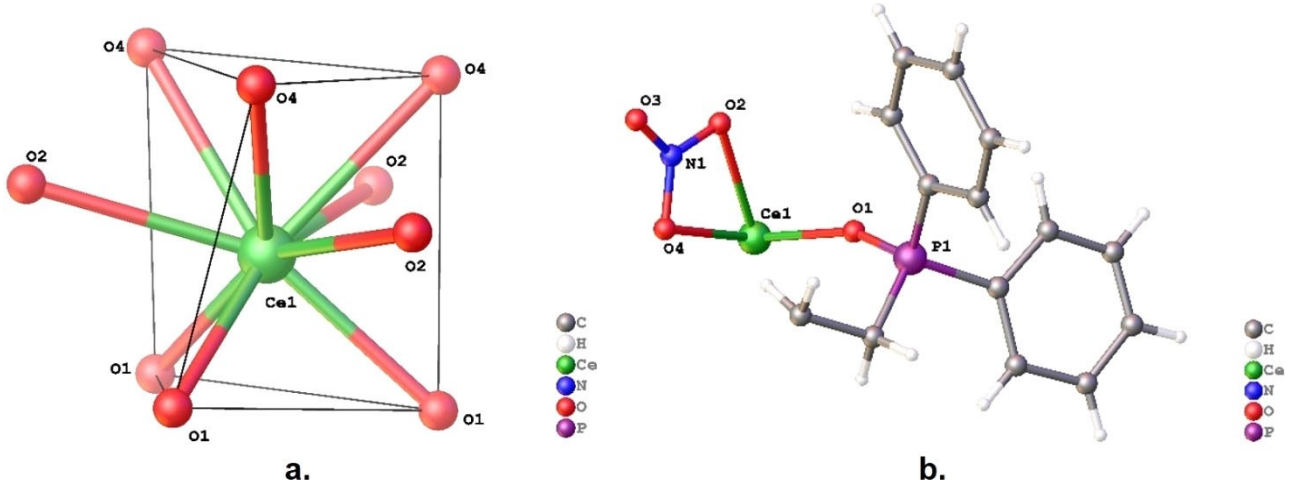

Figure 7. (a) The tricapped trigonal prismatic coordination geometry around the Ce ion in $Ce(NO_3)_3L^4_{1.5}$ (**5**). (b) The asymmetric unit with thermal ellipsoids drawn at the 50 % probability level.

the structure. The structure of (**5**) also differs from those of complexes of lanthanide(III) nitrates with L^4 produced by solvothermal synthesis which have dimeric structures with two $Ln(NO_3)_3L^4$ units, in which L^4 is chelating, bridged by a second L^4.[36] The difference in the structures could arise from the different methods of synthesis and the possible presence of Ce(IV). The cerium complex was not reported and so a direct comparison is not possible, however the praseodymium complex has been structurally characterised and as Pr^{3+} and Ce^{3+} have similar ionic radii some general comparisons between the two are meaningful. The Pr complex has a pseudo-*meridonal* coordination geometry again considering the nitrates again as monodentate ligands, whilst (**5**) has a pseudo-*facial* arrangement. In the Pr complex the *mer*-geometry gives rise to one *cis*-interaction between the chelating and bridging ligands. A *fac*-arrangement would lead to two such interactions and it is presumably this that leads to *meridonal* geometry being preferred in this case. In (**5**) the absence of chelating L^4 ligands means that the *fac*-geometry incurs no significant steric penalty and is preferred. Unusual differences in the metal oxygen bond distances are also found. From a consideration of the lanthanide contraction it would be expected that the Pr complex would have slightly smaller metal- oxygen distances whereas the opposite is the case, with the average Pr–O(N) 2.58(3) Å

© 2023 The Authors. European Journal of Inorganic Chemistry published by Wiley-VCH GmbH

10990682c, 0 Downloaded from https://chemistry-europe.onlinelibrary.wiley.com/doi/10.1002/ejic.202300375 by University Of Southampton, Wiley Online Library on [03/11/2023]. See the Terms and Conditions (https://onlinelibrary.wiley.com/terms-and-conditions) on Wiley Online Library for rules of use; OA articles are governed by the applicable Creative Commons License

Research Article
doi.org/10.1002/ejic.202300375

compared to Ce–O(N) 2.53(1) Å, and Pr–O(P) 2.38(2) Å Ce–O(P) 2.344(6) Å. Whilst it must be noted that this effect is small and the ranges of observed Ln–O distances for 9-coordinate Ce(III) and Pr(III) do overlap slightly,[29] it nonetheless implies Ce(IV) rather than Ce(III). The oxidation state calculations, however, give ambiguous results. This has previously been taken as being indicative of the presence of both Ce(III) and Ce(IV) in a structure,[28] although we can find no evidence of inequivalent Ce atoms in the structure. The elemental analysis gives a reasonable fit to the composition expected for Ce(IV) namely $[Ce(NO_3)_3L^4_{1.5}]^+[NO_3]^-$ for the bulk sample and on balance, whilst we cannot account for the oxidation state calculations, we favour the formulation as Ce(IV).

Solution properties and complex formation reactions

The isolated complexes of L^2, L^3 and L^4 have low solubility in common organic solvents and NMR spectra could be recorded in chlorocarbons and CD_3CN only with prolonged accumulation. The coordination shifts of the ^{31}P signals of all complexes are between 15–20 ppm to higher frequency of those of the free ligands. This is slightly lower than found for trialkylphosphine oxides, on coordination to Ce(IV) where coordination shift of around 25–30 ppm were observed.[18] This is probably because of the poorer donor ability of the aromatic substituted ligands studied here. The corresponding Ce(III) complexes all have ^{31}P NMR signals between 70–80 ppm due to the paramagnetic shift on coordination to the $4f^1$ centre.

$Ce(NO_3)_4L^1$ and $[Ce(NO_3)_2L^1_2][NO_3]$ (1) and (2)

The Ce(IV) and Ce(III) complexes of L^1 have reasonable solubility in organic solvents. The ^{31}P NMR spectrum of (**1**) in $CDCl_3$ shows a single sharp peak at 46.5 ppm ($W_{1/2}$ 6 Hz) shifted downfield from the position in the free ligand (29.8 ppm) as expected on coordination to the positively charged cerium centre. The spectrum of (**2**) is similarly as expected for a cerium(III) phosphine oxide complex with a significant paramagnetic shift.at 78.9 ppm. In both cases the addition of small quantities of L^1 to solutions of the complexes gave rise to spectra in which two separate peaks were seen at unchanged chemical shifts indicating that L^1 and its complexes do not undergo rapid exchange on the NMR timescale. Generally free monodentate phosphine oxides and their lanthanide complexes exchange rapidly in solution giving rise to a single signal. In this case the stronger binding with the bidentate ligands slows the exchange. In contrast to the complexes with more flexible ligand backbones which decompose to Ce(III) complexes (see below), (**1**) is relatively stable in solution, the ^{31}P NMR spectra showing no sign of decomposition to Ce(III) on standing for 14 days. Addition of methanol of $CDCl_3$ solution of (**1**) causes reduction of the Ce centre with formation of (**2**).

The formation of (**1**) was investigated by monitoring the reaction between an excess of CAN and L^1 in $CDCl_3$ and CD_3CN solutions. The reaction of an excess of solid CAN with an L^1 in $CDCl_3$ solution gave rise a yellow/orange solution within a few minutes of mixing, the ^{31}P NMR spectrum initially showed the signal from the free ligand to be absent and the presence of two peaks at 47.1 and 44.5 ppm in an approximately 1 : 4 ratio tentatively assigned as $Ce(NO_3)_4L^1$ and $Ce(NO_3)_4L^1_2$ respectively. The spectra are shown in Figure 8. The assignments of the predominant species initially formed as $Ce(NO_3)_4L^1_2$ is based on the presence of an excess of L^1 compared to soluble cerium in the initial stages of the reaction and on the ^{31}P NMR spectra of the isolated $Ce(NO_3)_4L^1$ and crude $Ce(NO_3)L^1_2$ complexes. An additional low intensity broad signal at 78.9 ppm was also observed and is assigned as $Ce(NO_3)_3L^1_2$ by comparison with the spectrum of an authentic sample. The large paramagnetic shift is typical for Ce(III) - phosphine oxide complexes. The Ce(III) complex is formed by reduction, probably from a small amount of residual $L^1 \cdot H_2O_2$ from the preparation of the ligand. On standing for 3 days the peak at 47.1 ppm due to $Ce(NO_3)_4L^1$ increased in intensity. This complex then reacts with the excess solid CAN present to give $Ce(NO_3)_4L^1$ as the major species in solution on standing.

The reactions of both $Ce(NO_3)_4L^1$ with added L^1, and of L^1 with increasing amount of CAN were studied in CD_3CN. The resulting spectra are shown in Figures 9a and 9b respectively. The same species as observed in $CDCl_3$ solution ($Ce(NO_3)_4L^1$ at 47.1 ppm and $Ce(NO_3)_4L^1_2$ at 45.3 ppm) were found and the presence of a further complex with a chemical shift of 44.7 ppm which increases in intensity at higher L^1 to Ce ratios and is probably a 1 : 3 complex which is in exchange with free ligand (broad signal at about 38 ppm).

The nature of the 1 : 2 complex is not certain from NMR measurements alone. It could possibly be a 12-coordinate neutral complex, but this seems unlikely in view of the presence of two bulky bidentate ligands and the ionic nature of the Ce(III) analogue. It seems, on balance more likely that this is an ionic complex, $[Ce(NO_3)_3L^1_2]^+$ which retains a 10-coordinate structure. Similarly the composition of the 1 : 3 complex is most likely to be ionic, possibly $[Ce(NO_3)_2L^1_3]^{2+}$ This was further investigated by a conductimetric titration of $Ce(NO_3)_4L^1$ (**1**) with L^1 in acetonitrile and the results are shown in Figure 10. The complex (**1**) is non conducting in CH_3CN indicating the same molecular structure in solution and solid state. On addition of L^1 the conductance increases giving a value in the range of a 1 : 1 electrolyte[37] at a 1 : 1 (**1**) : L^1 ratio. This indicates that $[Ce(NO_3)_3L^1_2]^+[NO_3]^-$ is the predominant species in solution. On increasing the proportion of L^1 the conductance increases to a value within the expected range of a 1 : 2 electrolyte suggesting that $[Ce(NO_3)_2L^1_3]^{2+} 2[NO_3]^-$ is formed. Thereafter the conductance does not rise sharply indicating that formation of the tricationic species $[Ce(NO_3)L^1_4]^{3+}$ $3[NO_3]^-$ only occurs to a small extent.

The reaction of aqueous CAN with L^1 in a 1 : 2 ratio in dichloromethane led to the isolation of an impure solid containing "$Ce(NO_3)_4L^1_2$" ($\delta = 44.6$ ppm) with a small amounts of (**2**) ($\delta = 78.6$ ppm) and L^1 ($\delta = 33.5$ ppm). Addition of solid CAN to a $CDCl_3$ solution of this solid gave rise to an additional signal at 46.7 ppm due to $Ce(NO_3)_4L^1$ which increased in intensity on

© 2023 The Authors. European Journal of Inorganic Chemistry published by Wiley-VCH GmbH

10990682c, 0 Downloaded from https://chemistry-europe.onlinelibrary.wiley.com/doi/10.1002/ejic.202300375 by University Of Southampton, Wiley Online Library on [03/11/2023]. See the Terms and Conditions (https://onlinelibrary.wiley.com/terms-and-conditions) on Wiley Online Library for rules of use; OA articles are governed by the applicable Creative Commons License

Research Article
doi.org/10.1002/ejic.202300375

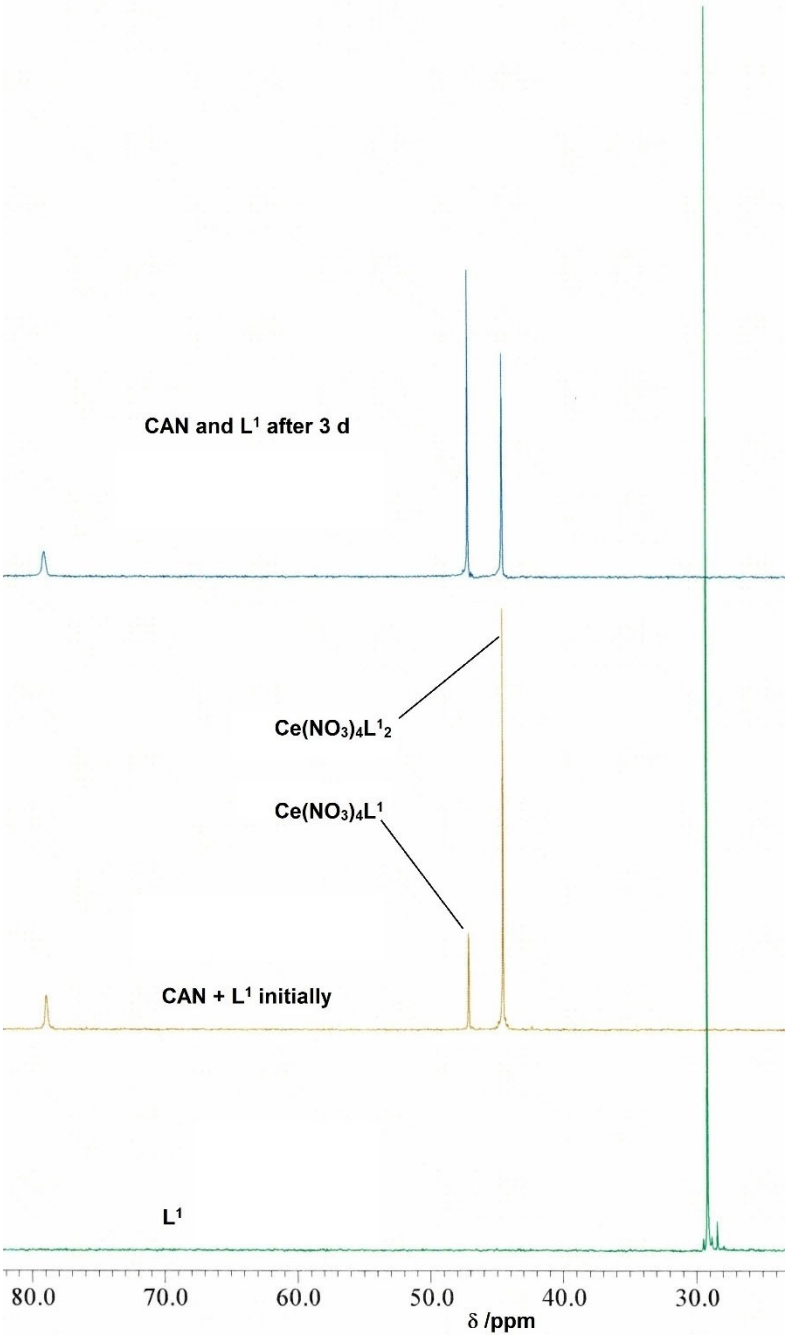

Figure 8. The evolution of the ^{31}P NMR spectra from the reaction of L^1 in $CDCl_3$ with excess solid CAN.

standing which is again consistent with the initial presence of the 1:2 complex.

$[Ce(NO_3)_3L^2_2]NO_3$ and $[Ce(NO_3)_2L^2_2]NO_3$

Impure $Ce(NO_3)_4L^2_2$ formed as a yellow powder and is poorly soluble in all common organic solvents. Whilst the substance is soluble in dimethylsulfoxide, the ^{31}P NMR spectrum in DMSO-d_6 gave a single sharp line at 24.2 ppm in good agreement with the shift of free L^2 showing that the complex undergoes complete ligand substitution in this solvent. The best solvent for NMR spectroscopy was CD_3CN in which spectra could be obtained with prolonged accumulation. The ^{31}P NMR spectrum shows two signals in a 1:1 ratio at 40.3 and 40.0 ppm assigned as $Ce(NO_3)_4L^2_2$ and a second lower intensity set of signals, again in a 1:1 ratio at 74.9 and 74.6 ppm due to $Ce(NO_3)_3L^2_2$ formed by decomposition. The assignment of the Ce(III) complex was confirmed by comparison with a sample prepared from $Ce(NO_3)_36H_2O$ and L^2 which had identical ^{31}P NMR and infrared spectra. On standing further decomposition to Ce(III) is evident with the Ce(III) complex present as the major species in solution

© 2023 The Authors. European Journal of Inorganic Chemistry published by Wiley-VCH GmbH

10990682c, 0 Downloaded from https://chemistry-europe.onlinelibrary.wiley.com/doi/10.1002/ejic.202300375 by University Of Southampton, Wiley Online Library on [03/11/2023]. See the Terms and Conditions (https://onlinelibrary.wiley.com/terms-and-conditions) on Wiley Online Library for rules of use; OA articles are governed by the applicable Creative Commons License

Research Article
doi.org/10.1002/ejic.202300375

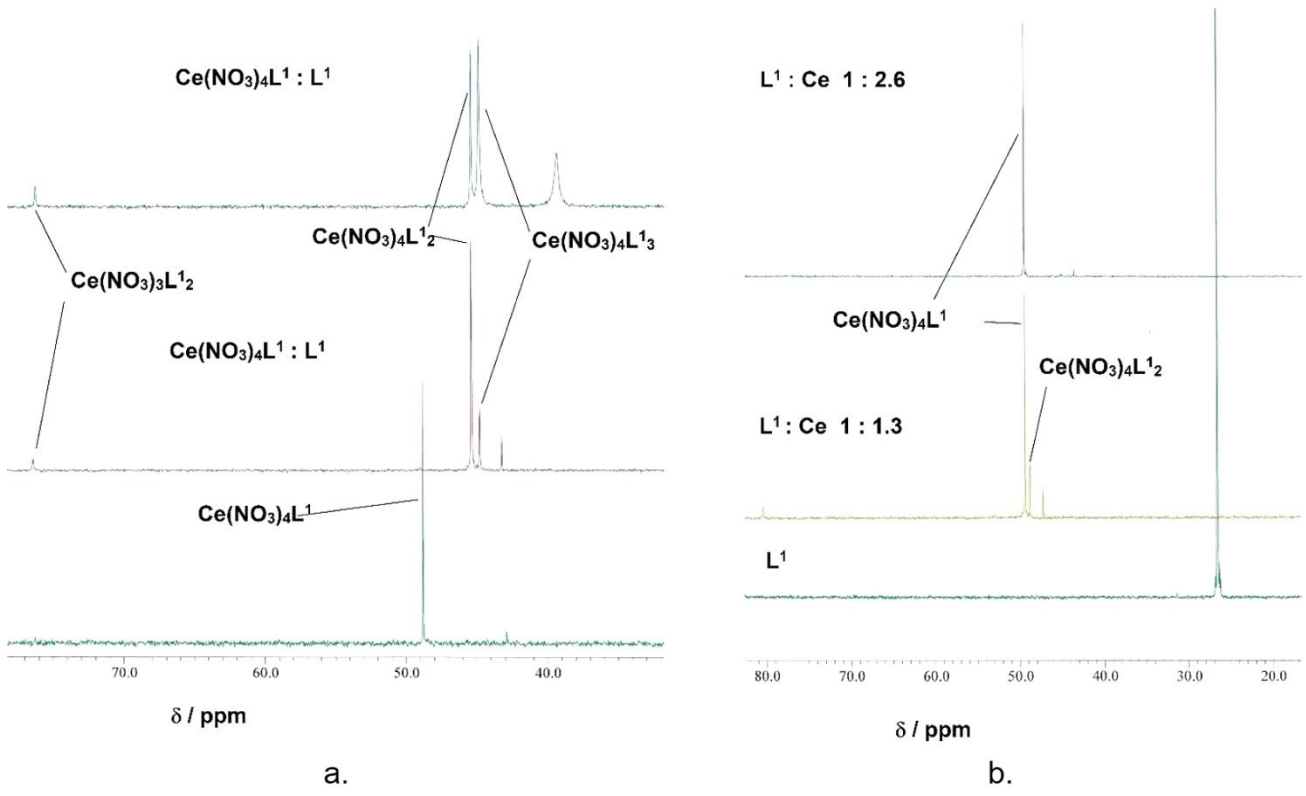

Figure 9. a. The 31P NMR spectra from a. $Ce(NO_3)_4L^1$ with increasing L^1 and b. L^1 with increasing amount of CAN in CD_3CN.

after standing for 5 d. After 14 d the decomposition is complete with the only signals present being due to the Ce(III) complex. Representative spectra are shown in Figure 11a. There are no other phosphorus containing species present in solution. Two sharp peaks in a 1:1 ratio suggest the presence of two inequivalent ligands within the complex which could be due to the ether oxygen atom in one of the ligands coordinating to Ce leading to two inequivalent phosphorus environments, possibly as an ionic complex $[Ce(NO_3)_3L^2_2]^+$ NO_3^-. At 80 °C the two signals from $Ce(NO_3)_4L^2_2$ coalesce to form a single sharp peak. This process is reversible, albeit with increased formation of Ce(III) with the same spectrum obtained on cooling to 25 °C as shown in Figure 11b There is precedent for L^2 acting as a tridentate ligand in the solid state in $[LnCl_2L^2_2]^+Cl^-$ which contain one bidentate and one tridentate ligand.[31]

The presence of two peaks for $Ce(NO_3)_3L^2_2$ could be explained in the same way, although in this case it must be noted that in the solid state structures of $[Ln(NO_3)_2L^2_2]^+[NO_3^-]$ (Ln = Pr, Lu) both the ligands are bidentate. In this case the variable temperature NMR spectra show a broadening of the signals but they do not coalesce at 80 °C indicating that the exchange between inequivalent sites is occurring but at a slower rate than in the Ce(IV) complex.

The investigation into the formation of complexes of L^2 in solution was hampered by the low solubility of the complexes in $CDCl_3$ and CD_3CN and of L^2 in CD_3CN. In both cases the reactions produced yellow poorly soluble materials. Depending on the solvent used, there are significant differences in the species formed which appear to be related to the solvent polarity. In polar solvents[38] such as CD_3CN two peaks in a 1:1 ratio are seen whilst the spectrum from the reaction between solid CAN with a $CDCl_3$ solution of L^2 gave spectra which showed the presence of excess L^2 together with a single peak at δ 44.0 and at 75.7 and 75.2 ppm for Ce(IV) and Ce(III) respectively. The simplest explanation is the ionisation of the complex in more polar solvents as indicated schematically in Figure 12. In CD_2Cl_2 a solvent with intermediate polarity a similar set of

spectra were obtained with two pairs of signals at 39.6 and 39.4 ppm for Ce(IV) and 74.9 and 74.2 ppm for Ce(III) and a single lower intensity peak at 44.7 ppm which is consistent with the unionised form with equivalent phosphorus environments being produced as observed in $CDCl_3$.

$[Ce(NO_3)_3L^3_2][NO_3]$ (3)

In CD_3CN the ^{31}P NMR spectrum of (**3**) shows two peaks, one at 51.8 ($W_{1/2}$ = 11 Hz) assigned to (**3**) and a lower intensity signal at 51.1 ppm in addition to abroad signal at 70.6 ppm ppm ($W_{1/2}$~300 Hz) due to Ce(III). On heating to 80 °C the signal due to (**3**) is considerably reduced in intensity with the major peak at 65.7 ppm due to a Ce(III) complex. On cooling this solution to ambient temperature only a single broad peak at 67 ppm ($W_{1/2}$ = 1.3 kHz) is observed indicating complete decomposition to Ce(III).

© 2023 The Authors. European Journal of Inorganic Chemistry published by Wiley-VCH GmbH

10990682c, 0 Downloaded from https://chemistry-europe.onlinelibrary.wiley.com/doi/10.1002/ejic.202300375 by University Of Southampton, Wiley Online Library on [03/11/2023]. See the Terms and Conditions (https://onlinelibrary.wiley.com/terms-and-conditions) on Wiley Online Library for rules of use; OA articles are governed by the applicable Creative Commons License

Research Article
doi.org/10.1002/ejic.202300375

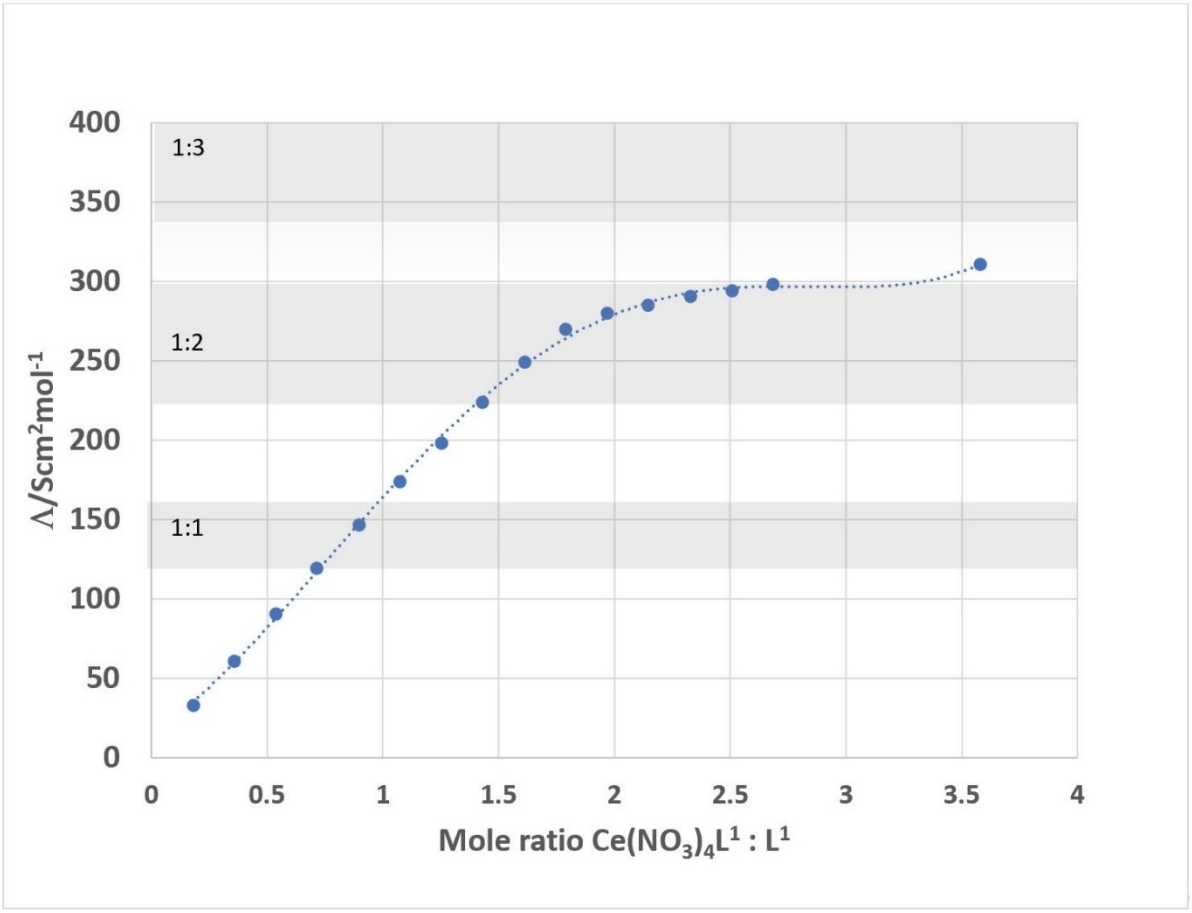

Figure 10. Molar conductance of an acetonitrile solution of (**1**) versus mole ratio of L^1. The accepted ranges for 1 : 1, 1 : 2 and 1 : 3 electrolytes are shown in the shaded areas.

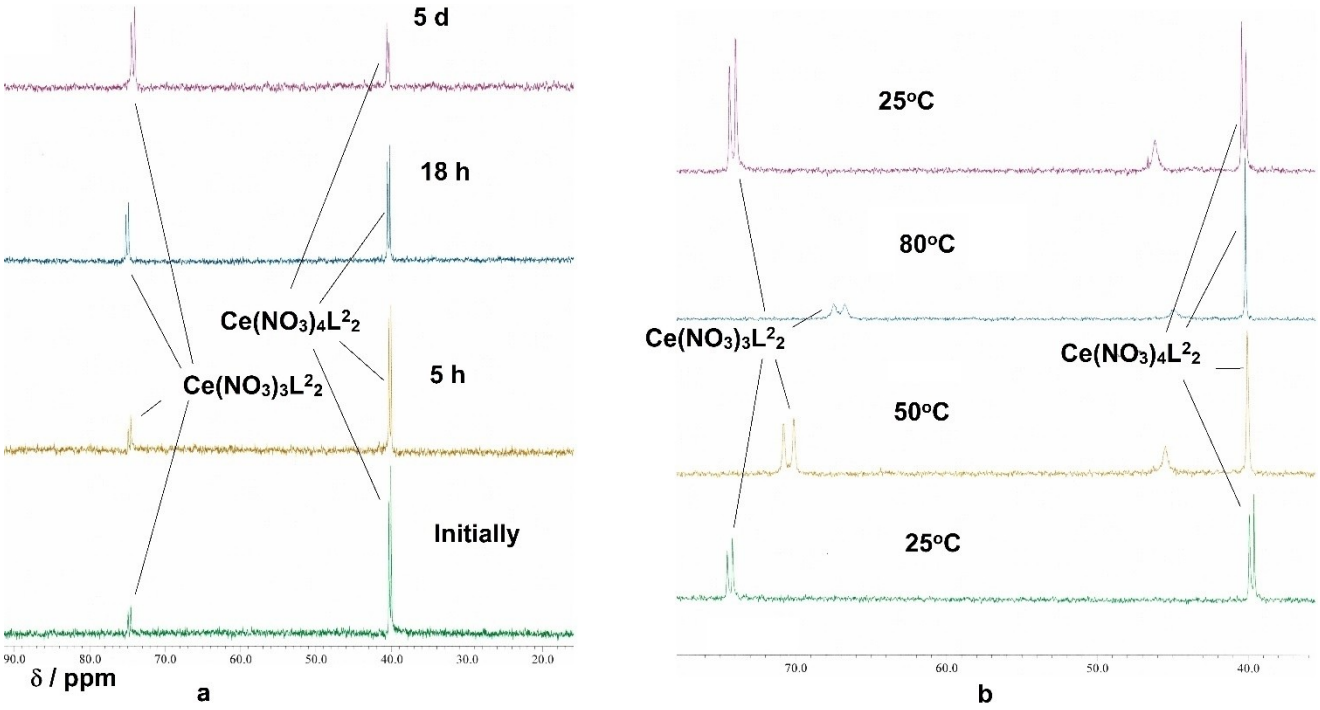

Figure 11. a. The decomposition of $Ce(NO_3)_4L^2_2$ to $Ce(NO_3)_3L^2_2$ b. The variable temperature ^{31}P NMR spectra in CD_3CN.

© 2023 The Authors. European Journal of Inorganic Chemistry published by Wiley-VCH GmbH

10990682c, 0 Downloaded from https://chemistry-europe.onlinelibrary.wiley.com/doi/10.1002/ejic.202300375 by University Of Southampton, Wiley Online Library on [03/11/2023]. See the Terms and Conditions (https://onlinelibrary.wiley.com/terms-and-conditions) on Wiley Online Library for rules of use; OA articles are governed by the applicable Creative Commons License

Research Article
doi.org/10.1002/ejic.202300375

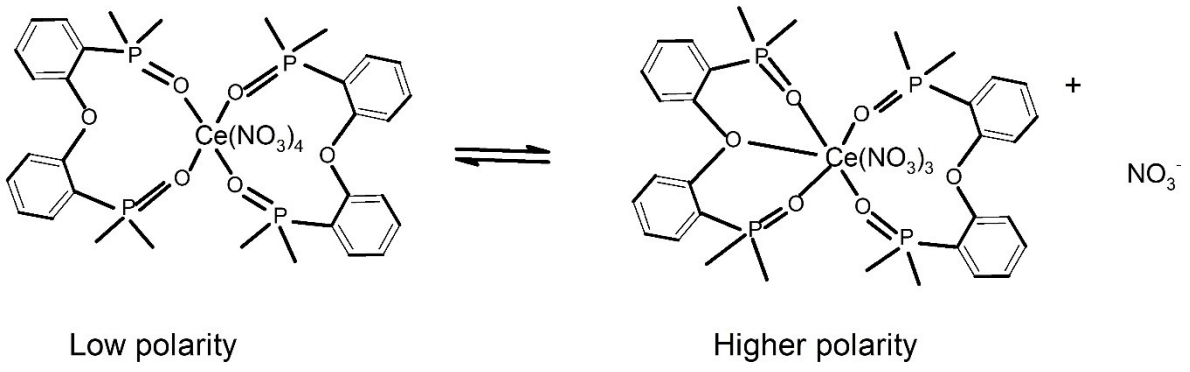

Figure 12. The probable speciation of complexes of L^2 with differing solvent polarity.

Investigations into the complex formation reaction in solution were hampered by, in addition to the insolubility of CAN in chlorocarbon solvents, the very low solubility of L^3 in CD_3CN. Addition of CAN to a suspension of L^3 in CD_3CN led to ^{31}P NMR spectra which showed a peak at 51.6 ppm assigned as $[Ce(NO_3)_3L^3_2]^+$ together with a lower intensity signal at 51.0 ppm which is tentatively assigned as a PO coordinated to Ce(IV), possibly $[Ce(NO_3)_2L^3_3]^{2+}$ on the basis of the ^{31}P chemical shift.

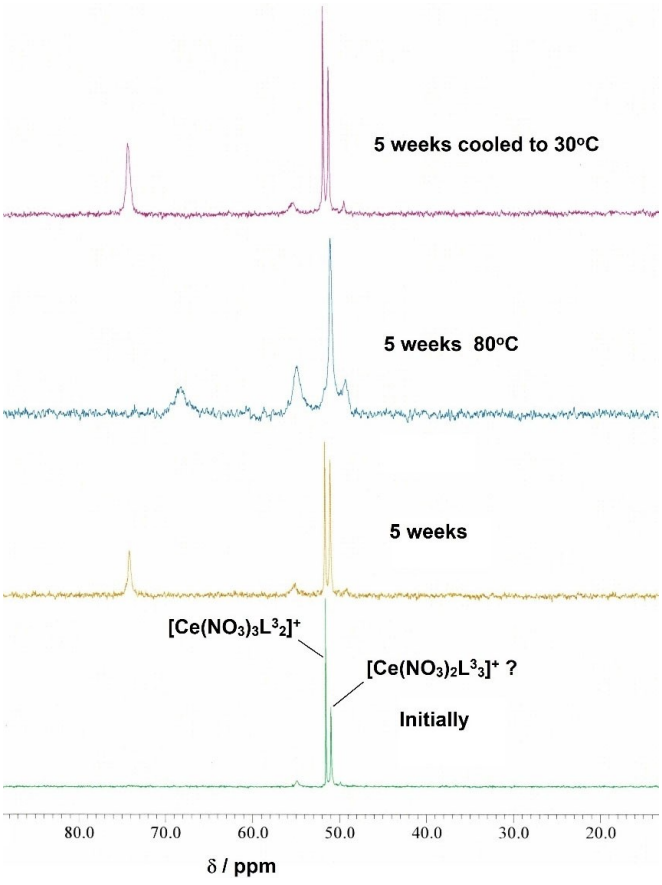

Figure 13. The ^{31}P NMR spectra of the L^3 CAN reaction in CD_3CN.

The evolution of the spectra over time is shown in Figure 13. The concentration of $[Ce(NO_3)_3L^3_2]^{2+}$ increases over 5 weeks as does the Ce(III) decomposition product.

At 80 °C the separate signals from the Ce(IV) complexes coalesce giving a single broad peak ($W_{1/2}$ = 70 Hz) indicating that the Ce(IV) complexes undergo rapid ligand exchange on the NMR timescale at 80 °C. On cooling to 30 °C two separate signals are again seen showing the process is reversible.

$Ce(NO_3)_3L^4_{1.5}$ (5)

The ^{31}P NMR spectrum of (**5**) in $CDCl_3$ shows several phosphorus environments. A small signal at 76.0 ppm is assigned as a Ce(III) complex and three peaks at 54.5, 53.0 and 50.1 ppm to Ce(IV). The spectrum is shown in Figure 14 and indicates that the solution structure differs from that in the solid state where all phosphorus atoms are equivalent. The reaction of L^4 in $CDCl_3$ with solid CAN with a Ce:L^4 ratio of 1:3 was slow. After 3 h the ^{31}P NMR spectrum showed a broadening of the L^4 signal to 80 Hz and a small broad peak ($W_{1/2}$ = ~600 Hz) assigned to a Ce(IV) complex at 53.3 ppm. After 2 weeks the intensity of the Ce(IV) species has increased significantly with an approximately 1:1 ratio of ligand (δ 33.4 $W_{1/2}$ = 180 Hz) and complex (δ 54.5 $W_{1/2}$ = 200 Hz) with a lower intensity signal at 50.1 ppm assigned to PO coordinated to Ce(IV).

The signals were both broad indicating exchange between free and bound ligand. On cooling to −30 °C the broad peaks in the region of 54 ppm resolved into three signals at 55.3, 54.4 and 52.0 ppm. In addition three low intensity broad resonances were seen at 101.5, 95.1 and 87.2 ppm, the low field shift and strong temperature dependence being characteristic of Ce(III) coordinated phosphine oxide. The behaviour of this system in solution is clearly more involved and the number of signals which can be assigned to Ce(IV) complexes on the basis of their chemical shifts indicates that a number of modes of bonding are occurring. By analogy with the solid state structures of trivalent lanthanides bonded to L^4[36] it is reasonable to suppose that here we are seeing the presence of both chelating and bridging L^4 in solution.

The reaction of L^4 with excess solid CAN in CD_2Cl_2 after 10 days showed a major peak at 54.6 ppm with a lower

© 2023 The Authors. European Journal of Inorganic Chemistry published by Wiley-VCH GmbH

10990682c, 0 Downloaded from https://chemistry-europe.onlinelibrary.wiley.com/doi/10.1002/ejic.202300375 by University Of Southampton, Wiley Online Library on [03/11/2023]. See the Terms and Conditions (https://onlinelibrary.wiley.com/terms-and-conditions) on Wiley Online Library for rules of use; OA articles are governed by the applicable Creative Commons License

Research Article
doi.org/10.1002/ejic.202300375

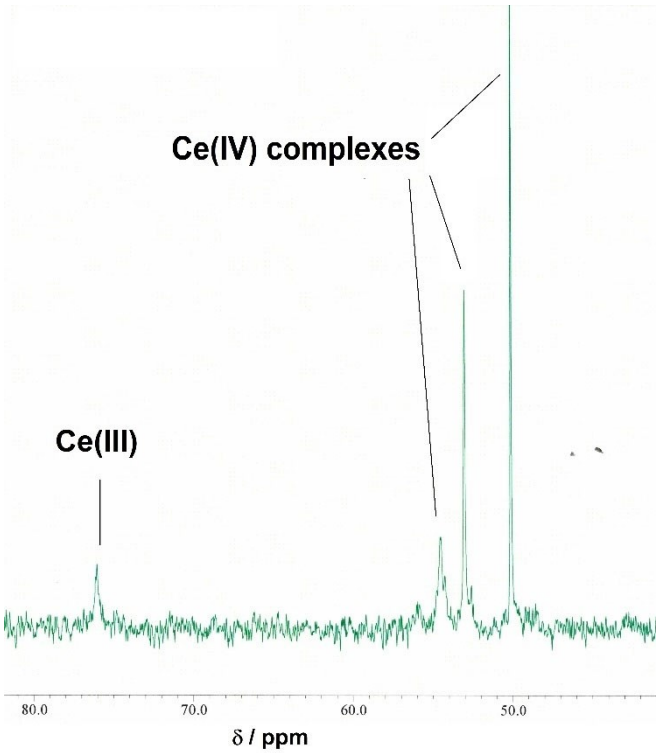

Figure 14. The ^{31}P NMR spectrum of (**5**) in $CDCl_3$.

intensity signal at 50.5 ppm, both assigned as Ce(IV). There was little evidence for the formation of Ce(III) in solution over this time.

Investigation of the reactions in CD_3CN and in CD_3NO_2 was again hampered by the very low solubility of L^4 in these solvents. The reaction carried out with a suspension of L^4 with a solution of CAN in CD_3CN (effectively the reaction of L^4 with an excess of CAN) led to the dissolution of L^4 and a ^{31}P NMR spectrum which showed the presence of two Ce(IV) species at 57.1 ppm(major) and 51.9 ppm(minor). Similar results were obtained when using CD_3NO_2 (δ 57.2 major and δ 52.1 minor) which closely correspond to the spectrum obtained from CD_2Cl_2. On heating at 90 °C for 6 h some decomposition to Ce(III) was evident with a low intensity broad signal at about 70 ppm moving to 78 ppm at 30 °C.

Conclusions

The reactions of CAN with L^1 led to the isolation of a 1:1 molecular complex (**1**) which is stable in solution with strong evidence for the formation (^{31}P NMR and conductance measurements) of ionic species, $[Ce(NO_3)_3L^1_2]^+$ and $[Ce(NO_3)_2L^1_3]^{2+}$ and possibly $[Ce(NO_3)L^1_4]^{3+}$, formed in solution on addition of further L^1. Reaction with $Ce(NO_3)_3{\cdot}6H_2O$ led to the formation of the ionic $[Ce(NO_3)_2L^1_2]^+[NO_3]^-$. The reactions of CAN with L^2 formed less stable complexes which decompose to Ce(III) in solution. With L^3 the ionic $[Ce(NO_3)_3L^3_2]^+$ (**3** and **4**) was formed. There is evidence for the formation of further Ce(IV) complexes in solution, possibly $[Ce(NO_3)_2L^3_2]^{2+}$. In solution decomposition to Ce(III) occurs. For L^4 the polymeric complex, $[Ce(NO_3)_3L^4_{1.5}]_n n$-$[NO_3]^-$ (**5**) was isolated. In solution the presence of signals from both Ce(IV) and Ce(III) indicate that complexes of L^2, L^3 and L^4 are less stable than those of L^1. The marked contrast in stability of the Ce(IV) complexes could be correlated with the flexibility of the ligand backbones with the more rigid L^1 forming the most stable complexes.

In the solid state cerium(IV) complexes of L^1 are less thermally stable than the Ce(III) analogue and more stable than the complex with L^2. The increased solid state stability of (**1**) compared to (**3**) mirrors the solution stabilities.

Experimental Section

NMR spectra were recorded in $CDCl_3$ solution on a JEOL ECX 400, approximately 20 mg of solid in 1 mL of the appropriate deuterated solvent.

Thermogravimetric Analysis was carried out using a Perkin Elmer TGA 8000 set with a balance purge of 60 ml/min and sample purge of 40 ml/min nitrogen. The initial temperature was set to 50 °C and held for 1 min, the temperature was raised to 1000 °C at a rate of 10 °C/min and then held for 1 min.

The evolved gases were collected from the TGA and transferred to a Perkin Elmer Spectrum 2 FTIR fitted with a gas cell by a heated (270 °C) transfer line using nitrogen as carrier gas at a flow of 80 ml/min. The FTIR continuously collected data throughout the TGA analysis with a resolution of 8 cm^{-1} and 4 scans.

Infrared spectra were recorded with a resolution of ± 2 cm^{-1} on a Thermo Nicolet Avatar 370 FT-IR spectrometer operating in ATR mode. The samples were compressed onto the optical window and spectra recorded without further sample pre-treatment.

X-ray Crystallography: Suitable crystals of each compound were selected, coated in protective perfluoroether oil, and mounted on a MiTeGen holder. Diffraction data were collected on a Rigaku FRE+ diffractometer equipped with VHF Varimax confocal mirrors and an AFC12 goniometer and HyPix 6000HE detector (Compounds (**1**) and (**2**)) or a Rigaku 007HF equipped with Varimax confocal mirrors and an AFC11 goniometer and HyPix 6000 detector (Compounds (**3**), (**4**), and (**5**)). The crystals were kept at a steady $T = 100(2)$ K during data collection. The structure was solved with the **ShelXT**[39] structure solution program using the Intrinsic Phasing solution method and by using **Olex2**[40] as the graphical interface. The model was refined with version 2014/7 of **ShelXL**[39]) using Least Squares minimisation. The total number of runs and images was based on the strategy calculation from the program **CrysAlisPro**.[41] Low angle reflections that were affected by the beamstop have been omitted from the refinement. All non-hydrogen atoms were refined with anisotropic thermal displacement parameters. Aromatic and aliphatic hydrogen atoms have been included at their geometrically estimated positions. Hydrogen atoms bound to disordered water molecules, and the hydroxyl hydrogen atoms of disordered ethanol molecules, could not be located in the difference map, and would not converge into a preferred orientation when included at geometrically estimated positions. These hydrogen atoms have been omitted from the final model, but included in the final molecular formula. Model refinement was unremarkable, except in the following instances. Further details may, in all cases, be found in the cifs.

© 2023 The Authors. European Journal of Inorganic Chemistry published by Wiley-VCH GmbH

10990682c, 0 Downloaded from https://chemistry-europe.onlinelibrary.wiley.com/doi/10.1002/ejic.202300375 by University Of Southampton, Wiley Online Library on [03/11/2023]. See the Terms and Conditions (https://onlinelibrary.wiley.com/terms-and-conditions) on Wiley Online Library for rules of use; OA articles are governed by the applicable Creative Commons License

(**2**): Elongated thermal ellipsoids of the atoms of the aromatic ring containing C73 indicated that the ring is disordered, and has been modelled over two sites of complementary occupancies.

(**3**) and (**4**): The non-coordinated nitrate anion was found to be disordered, and has been modelled over two sites, with 55% and 45% occupancy. In (**3**) only, a further peak close to O10 N has been modelled as the oxygen atom of a 45% occupancy water molecule. Elongated thermal ellipsoids of the atoms of the rings containing C15, C21, and C27 indicated that these rings were disordered, and they have each been modelled over two sites with complementary occupancies. Large peaks of residual electron density indicated the presence of disordered, partial occupancy chloroform molecule that essentially create a one directional smear of electron density. No attempt was made to resolve this disorder. A solvent mask has been applied, and the presence of approximately 2.25 molecules of $CHCl_3$ (**3**) or CD_2Cl_2 (**4**) were calculated to occupy the void space.

(**5**) Only the 3 coordinated nitrate anions could be located, and the poor resolution of the diffraction data did not allow for reliable oxidation state determination of the Ce centre. There are some cavities available for solvents (129 $Å^3$ per asymmetric unit). No solvent molecules could be identified, and a solvent mask was applied (more details may be found in the solvent mask section of the cif), giving a calculated electron count consistent with the presence of one nitrate anion and 1.75 CH_2Cl_2 molecules per Ce centre. The nitrate anion and CH_2Cl_2 molecules calculated by the solvent mask have not been modelled but have been included in the final molecular formula. R_{int} is somewhat high, which is most likely because the I = odd reflections are very weak. Attempts to solve this structure with $c = 11.1$ Å were unsuccessful. Given that a cerium (IV) salt was used to prepare this material, it has been assumed for molecular formula

Deposition Number(s) 2263571-2263575 (for **5**, **1**, **2**, **4** and **3**) contain(s) the supplementary crystallographic data for this paper. These data are provided free of charge by the joint Cambridge Crystallographic Data Centre and Fachinformationszentrum Karlsruhe Access Structures service.

Synthesis: $Ce(NO_3)_4L^1$ (**1**) An excess of ceric ammonium nitrate, $(NH_4)_2Ce(NO_3)_6$ (0.92 g 1.68 mmol) was added to a solution of L^1 (0.27 g 0.45 mmol) in 4.5 ml dichloromethane and the mixture stirred for 24 h to give a dark brown suspension. The suspension was filtered to give a dark brown solution which was cooled to −30 °C. The dark brown crystals which formed were filtered, washed with a small quantity of dichloromethane and dried at the pump to give $Ce(NO_3)_4L^1$ (0.37 g 84% based on L^1). Infrared/cm^{-1} (ATR) 1516(s), 1507(s) (N–O), 1276(m), 1262 (s), 1247(s), 1229(s) (N–O), 1100(s) (P=O).

Analysis: required (found) C47.66(47.01), H3.28(2.90), N5.70(5.46)

$[Ce(NO_3)_2L^1{}_2][NO_3]\cdot EtOH$ (**2**) $Ce(NO_3)_3\cdot 6H_2O$ 0.22 g (0.5 mmol) was dissolved in 2.5 ml warm ethanol and a solution of 0.62 g (1.0 mmol) L^1 in 7.5 ml warm ethanol was added to give a white precipitate. The mixture digested on a steam bath for 30 minutes after which it was cooled to room temperature, filtered, washed with ethanol and dried to give 0.66 g (84%) colourless crystals.

Analysis: required (found) 60.54(60.17), H4.17(4.02), N2.71 (2.57)

$[Ce(NO_3)_4L^3\cdot 2CHCl_3$ A solution of an excess of ceric ammonium nitrate (0.43 g 0.78 mmol) in 2.5 ml water was stirred with a solution of L^3 (0.25 g 0.58 mmol) in chloroform (1.2 ml). The stirring was continued for 30 minutes. The dark red lower layer was separated and dried ($MgSO_4$). Dark brown crystals of the title complex formed on standing overnight and were filtered and dried at the pump to give 0.24 g Infrared/cm^{-1} (ATR) 1507(m)(N–O), 1271(m)(N–O), 1069(s)(P=O), 953(w)(N–O).

Analysis: required (found) C43.60(43.53), H3.38(3.42), N3.77(3.94)

$Ce(NO_3)_4L^4{}_{1.5}\cdot[NO_3]$ Solid ceric ammonium nitrate (46.4 mg 0.08 mmol) was added to a solution of L^4 (24.6 mg 0.05 mmol) in CD_2Cl_2 (0.5 ml) in a 5 mm o.d. nmr tube. After 14 d the solution was decanted from undissolved solid. Slow evaporation of the solution to a small volume led to the formation of a small quantity of orange crystals. Infrared/cm^{-1} (ATR) 1528(m), 1458(m)(N–O), 1282(m)(N–O), 1141(s), 1123(s)(P=O), 952(w)(N–O).

Analysis: required (found) C46.89(46.80), H3.95(4.21), N5.21(4.74)

Acknowledgements

We are grateful to the EPSRC for the use of the National Crystallography Service at Southampton University.[42]

Conflict of Interests

The authors declare no conflict of interest.

Data Availability Statement

The data that support the findings of this study are available from the corresponding author upon reasonable request.

Keywords: Cerium · coordination complexes · NMR spectroscopy · thermogravimetry · X-ray diffraction

[1] H. Feuchter, S. Duval, C. Volkringer, F.-X. Ouf, L. Rigollet, L. Cantrel, M. De Mendonca Andrade, F. Salm, C. Lavalette, T. Loiseau *ACS Omega* **2019**, *4 (7)*, 12896–12904.
[2] J. Zhang, M. Wenzel, K. Schnaars, F. Hennersdorf, K. Schwedtmann, J. März, A. Rossberg, P. Kaden, F. Kraus, T. Stumpfb, J. J. Weigand, *Dalton Trans.* **2021**, *50*, 3550–3558.
[3] H. Tsurugi, K. Mashima, *J.Amer. Chem. Soc.* **2021**, *143 (21)*, 7879–7890.
[4] Q. An, Z. Wang, Y. Chen, X Wang, K. Zhang, H. Pan, W. Liu, Z. Zuo, *J. Am. Chem. Soc.* **2020**, *142 (13)*, 6216–6226.
[5] K. Zhang, L. Chang, Q. An, X. Wang, Z. Zuo, *J.Amer. Chem. Soc.* **2019**, *141* 10556–10564.
[6] Y. Qiao, E. J. Schelter, *Acc. Chem. Res.* **2018**, *51*, 2926–2936.
[7] C. J. Slevin, J. Zhang, P. R. Unwin, *J. Phys. Chem. B* **2002**, *106*, 3019–3025.
[8] H. Mehdi, A. Bodor, D. Lantos, I. T. Horvath, D. E. De Vos, K. Binnemans, *J. Org. Chem.* **2007**, *72*, 517–524.
[9] A. Deepthi, *Chem. Rev.* **2007**, *107*, 1862–1891.
[10] M. Huang, Y. Fu, Y. Lu, W. Liao, Z. Li, *J. Rare Earth* **2020**, *38*, 1330–1336.
[11] A. W. G. Platt, *Coord. Chem. Rev.* **2017**, *340*, 62–78.
[12] Y.-M. So, W.-H. Leung, *Coord. Chem. Rev.* **2017**, *340*, 172–197.
[13] M. Ul-Haque, C. N. Caughlin, F. A. Hart, R. Van Nice, *Inorg. Chem.* **1971**, *10*, 115–122.
[14] J. Lin, E. Hey-Hawkins, H. G. von Schnering, *Z. Naturforsch.* **1990**, *45a*, 1241–1247.
[15] R. Babecki, A. W. G. Platt, R. R. Russell, *Inorg. Chim. Acta* **1990**, *171*, 25–28.
[16] Y. Koide, A. Sakamoto, T. Imamoto, T. Tanase, Y. Yamamoto, *J. Alloys Compd.* **1993**, *192* 211–216.
[17] P.-Y. Jiang, Y. Ikeda, M. Kumagai, *J. Nucl. Sci. Technol.* **1994**, *31*, 491–493.
[18] S. J. Coles, S. J. Fieldhouse, W. T. Klooster, A. W. G. Platt, *Polyhedron* **2019**, *16*, 1346–351.
[19] K. Nakamoto, *Infrared and Raman Spectra of Inorganic and Coordination Compounds*, 5th Ed, Wiley **1997**.
[20] O. Ito, S. Akiho, M. Iino, *J. Phys. Chem.* **1989**, *93*, 4079–4083.

© 2023 The Authors. European Journal of Inorganic Chemistry published by Wiley-VCH GmbH

10990682c, 0 Downloaded from https://chemistry-europe.onlinelibrary.wiley.com/doi/10.1002/ejic.202300375 by University Of Southampton, Wiley Online Library on [03/11/2023]. See the Terms and Conditions (https://onlinelibrary.wiley.com/terms-and-conditions) on Wiley Online Library for rules of use; OA articles are governed by the applicable Creative Commons License

Research Article
doi.org/10.1002/ejic.202300375

[21] N. Guillou, J. P. Auffrdic, D. Louer, *J. Solid State Chem.* **1995**, *115*, 925–298.
[22] N. Guillou, J. P. Auffredic, D. Louer, *J. Solid State Chem.* **1996**, *122*, 59–67.
[23] S. Yuvaraj, L. Fan-Yuan, C. Tsong-Huei, Y. Chuin-Tih, *J. Phys. Chem. B* **2003**, *107*, 1044–1047.
[24] T.-J. Lin, C.-C. Chiu, *Phys. Chem. Chem. Phys.* **2018**, *20*, 345–356.
[25] E. L. Elzinga, D. L. Sparks, *J. Coll. Interface Sci.* **2007**, *308*, 53–70.
[26] S. Alvarez, P. Alemany, D. Casanova, J. Cirera, M. Llunell, D. Avnir, *Coord. Chem. Rev.* **2005**, *249*, 1693–1708.
[27] M. Llunell, D. Casanova, J. Cirera, P. Alemany, S. Alvarez, SHAPE – Program for the Stereochemical Analysis of Molecular Fragments by Means of Continuous Shape Measures and Associated Tools, Version 2.1, University of Barcelona, Spain, **2013** Shape.
[28] G. J. Palenik, S.-Z. Hu, *Inorg. Chim. Acta* **2009** *362*, 4740–4743.
[29] O. C. Gagné, *Acta Crystallogr.* **2018**, *B74*, 49–62.
[30] B. Deb, D. K. Dutta, *Polyhedron* **2009**, *28*, 2258–2262.
[31] J. Fawcett, A. W. G. Platt, S. V ickers, M. D. Ward, *Polyhedron* **2004**, *23*, 2561–2567.
[32] K. Miyata, T. Nakagawa, R. Kawakami, Y. Kita, K. Sugimoto, T. Nakashima, T. Harada, T. Kawai, Y. Hasegawa, *Chem. Eur. J.* **2011**, *17*, 521–528.
[33] D. B. Ambili Raj, B. Francis, M. L. P. Reddy, R. R. Butorac, V. M. Lynch, A. H. Cowley, *Inorg. Chem.* **2010**, *49*, 9055–9063.
[34] Z. Spichal, M. Necas, J. Pinkas, J. Noosad, *Inorg. Chem.* **2004**, *43*, 2776–2778.
[35] E. Bonfada, E. Schulz-Lang, R. A. Xan, U. Abrram, *Z. Naturforsch. B* **2014**,*55*, 285–290.
[36] Z. Spichal, M. Necas, J. Pinkas, Z. Zdrahal, *Polyhedron* **2006**, *25*, 809–814.
[37] W. J. Geary, *Coord. Chem. Rev.* **1971**, *7*, 81–122.
[38] C. Reichardt, *Solvents and Solvent Effects in Organic Chemistry*, Wiley-VCH, 3rd ed., **2003**.
[39] G. M. Sheldrick, *Acta Crystallogr.* **2015**, *C27*, 3–8; G. M. Sheldrick, ShelXT- *Acta Crystallogr.* **2015**, *A71*, 3–8.
[40] O. V. Dolomanov, L. J. Bourhis, R. J. Gildea, J. A. K. Howard, H. Puschmann, *J. Appl. Crystallogr.* **2009**, *42*, 339–341.
[41] CrysAlisPro Software System, Rigaku Oxford Diffraction, (**2019**).
[42] S. J. Coles, P. A. Gale, *Chem. Sci.* **2012**, *3*, 68.

Manuscript received: June 15, 2023
Revised manuscript received: July 12, 2023
Accepted manuscript online: July 24, 2023
Version of record online: ■■, ■■

© 2023 The Authors. European Journal of Inorganic Chemistry published by Wiley-VCH GmbH

10990682c, 0 Downloaded from https://chemistry-europe.onlinelibrary.wiley.com/doi/10.1002/ejic.202300375 by University Of Southampton, Wiley Online Library on [03/11/2023]. See the Terms and Conditions (https://onlinelibrary.wiley.com/terms-and-conditions) on Wiley Online Library for rules of use; OA articles are governed by the applicable Creative Commons License

RESEARCH ARTICLE

The formation, structures and thermal and solution stability of cerium(IV) complexes with bidentate phosphine oxides are reported. Complexes with flexible ligand architecture tend to be less stable showing decomposition to Ce(III) in solution. The decomposition products of the thermal decomposition in the solid state have been identified by infrared spectroscopy.

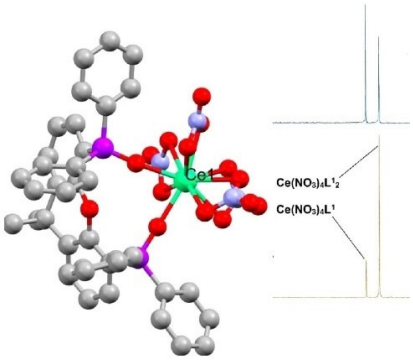

*Prof. S. J. Coles, S. Cooper, Dr. W. T. Klooster, Dr. L. J McCormick Mc Pherson, Dr. A. W. G. Platt**

10990682c, 0, Downloaded from https://chemistry-europe.onlinelibrary.wiley.com/doi/10.1002/ejic.202300375 by University Of Southampton, Wiley Online Library on [03/11/2023]. See the Terms and Conditions (https://onlinelibrary.wiley.com/terms-and-conditions) on Wiley Online Library for rules of use; OA articles are governed by the applicable Creative Commons License